

Towards the glueball spectrum of full QCD*

SESAM collaboration: G.S. Bali^a, U. Glässner^b, S. Güsken^b, H. Hoerber^c, Th. Lippert^c, G. Ritzenhöfer^c, K. Schilling^{b,c}, G. Siegert^c and A. Spitz^b

^aDepartment of Physics, The University, Highfield, Southampton SO17 1BJ, UK

^bPhysics Department, University of Wuppertal, D-42097 Wuppertal, Germany

^cHLRZ c/o Forschungszentrum Jülich, D-52425 Jülich, and DESY, D-22603 Hamburg, Germany

We present first results on masses of the scalar and tensor glueballs as well as of the torelon from simulations of QCD with two light flavours of Wilson fermions. The gauge configurations of extent $16^3 32$ at $\beta = 5.6$ and $\kappa = 0.156, 0.157$ and 0.1575 have been generated as part of the SESAM collaboration programme. The present lattice resolutions correspond to $a^{-1} = 2.0\text{--}2.3$ GeV and ratios $m_\pi/m_\rho \approx 0.83, 0.76$ and 0.71 , respectively. Studies on larger lattice volumes and closer to the chiral limit are in progress.

1. INTRODUCTION

Recently, increased attention has been paid on lattice glueball computations [1,2]. It is demanding to include sea quarks into such studies as two new effects are expected to set in: the scalar glueball becomes unstable and can decay into two π 's (at sufficiently light sea quark mass). Also, mixing with mesonic $I = 0$ states might occur. In this case, the glueball will just add an additional excitation to the singlet state of the $L = 1$, $J^{PC} = 0^{++}$ meson quartet (nonet in full QCD with three light flavours of sea quarks), which does not fit into the constituent quark model. In fact, one can equally well speak of a meson with valence quarks and sea glue as of a glueball with valence glue and sea quarks. Only the couplings to certain decay channels can discriminate which of these two features dominates in either state. Depending on the quark masses, a glueball creation operator will project onto all these states ($\pi\pi$ and mixed meson-glue states). One aim of the present study is to look for unexpected or dramatic effects around such thresholds.

In addition to glueballs, we study so called torelon states, i.e. flux tubes wrapping around the lattice (with periodic spatial boundary con-

ditions). In case of the valence quark approximation, the mass of such a state is (up to finite size corrections) expected to equal $L_S a \kappa$ where L_S denotes the spatial extent of the lattice (here: $L_S = 16$) and $\kappa = K/a^2$ stands for the string tension. When dynamical sea quark flavours are switched on, the lightest such state (A_{1g}) can, at sufficiently large lattice extent, decay into either a scalar meson or into two π 's or mix with glueball states through intermediate mesonic states. In the torelon we expect to be sensitive to "string breaking" effects.

It is well known from quenched studies that gluonic observables suffer from large statistical fluctuations and small signals [1–3]. Early studies with staggered sea quarks [4] indicate that it might be extremely difficult to obtain significant results on glueballs with dynamical fermions at all in realistic time. In view of the interesting physics involved, we wish to explore the situation with our medium size sample of configurations.

2. METHOD

We compute matrices of zero-momentum projected plaquette-plaquette and Wilsonline-Wilsonline correlators at various fuzzing levels [3]. Two different fuzzing procedures have been applied for this purpose:

1. successive factor two blocking [3] with the

*Presented by G. Bali at Lattice '96, International Symposium on Lattice Field Theory, St. Louis, USA, June 4 – 8, 1996.

straight connection weighted by a coefficient $\alpha = 1$, in respect to the neighbouring four spatial staples,

2. alternating between conventional APE smearing steps with $\alpha = 4$ (keeping the length of the fuzzed link constant) and the above factor two blocking steps.

Within procedure 1, the fuzzing levels are labeled by $n = 1, \dots, 3$, corresponding to links of effective length 2^n in lattice units. Within procedure 2, two successive levels correspond to fuzzed links of equal length, i.e. levels 0 and 1 yield links of extent 1 while 6 and 7 yield links of length 8.

Procedure 1 has been applied onto 2196 successive trajectories at $\kappa = 0.157$, $V = 16^3 32$, $\beta = 5.6$ while procedure 2 has so far been applied to 204, 274 and 260 configurations, separated by about 10 trajectories, at $\kappa = 0.156$, $\kappa = 0.157$ and $\kappa = 0.1575$, respectively. Prior to statistical analysis the data has been binned into sufficiently large blocks to achieve stability of the error estimates in respect to the block size, i.e. to avoid autocorrelations. Statistical errors have been computed from the scatter between 500 bootstrap samples in either case.

Operators with quantum numbers A_{1g} (the lightest torelon state), T_1^{++} (projecting onto the $J^{PC} = 0^{++}$ glueball) and E^{++} (2^{++}) have been constructed at each fuzzing level. After diagonalizing the 2×2 submatrix between the two basis states with best ground state overlap in each case, masses of the glueball and torelon states are extracted.

Applying fuzzing procedure 1, levels 2 and 3 have been found to project best onto the glueball ground states while just level 3 resulted in a satisfying overlaps for the torelon case. For fuzzing 2, levels 6 and 5 (7 and 6 for the torelon) are optimal. After diagonalizing the corresponding correlation submatrices, we obtain ground state overlaps of $72 \pm 7\%$ for the 0^{++} glueball and $70 \pm 9\%$ for the torelon by use of fuzzing 1. With procedure 2, glueball overlaps of $71 \pm 6\%$, $81 \pm 5\%$ and $79 \pm 5\%$ and torelon overlaps of $93 \pm 8\%$, $98 \pm 6\%$ and $89 \pm 4\%$ have been achieved for the three κ values, respectively, resulting in an earlier onset of plateaus in local masses and, thus, reduced sta-

tistical errors of final results.

3. RESULTS

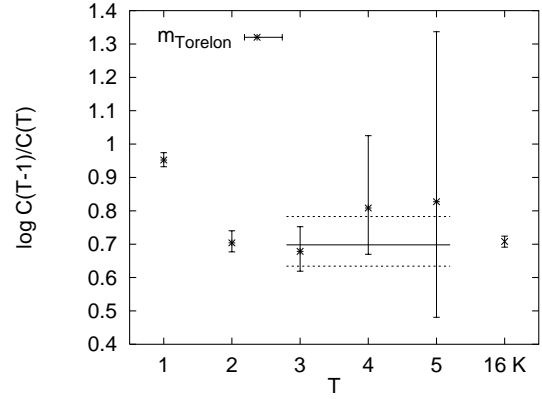


Figure 1. Torelon effective mass (fuzzing procedure 1). The rightmost point is the expectation from the static potential.

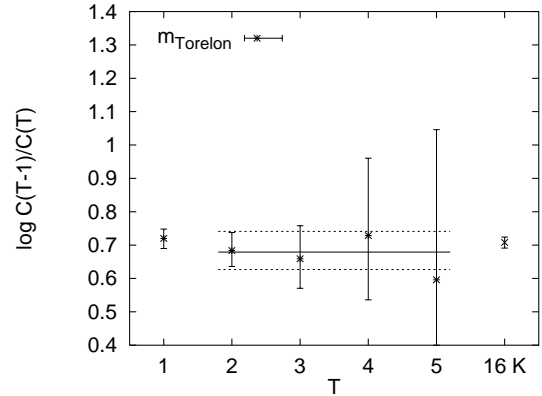


Figure 2. Torelon effective mass (fuzzing procedure 2).

In Figs. 1 and 2 we compare our results for the torelon mass at $\kappa = 0.157$ from the two fuzzing procedures. The numerical values are $M(A_{1g}) = 0.698^{+85}_{-65}$ and 0.679^{+62}_{-52} , in agreement

with an expectation of $16K = 0.712^{+16}_{-17}$, as computed from the linear slope of the interquark potential [5]. Note, that the leading order finite size effect, $\pi/(3L_S^2) \approx 0.004$, is small.

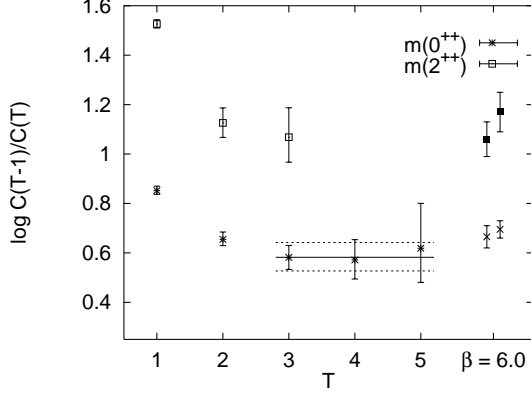


Figure 3. Effective glueball masses (fuzzing procedure 1). The rightmost data points are expectations from quenched simulations at $\beta = 6.0$ [3,6].

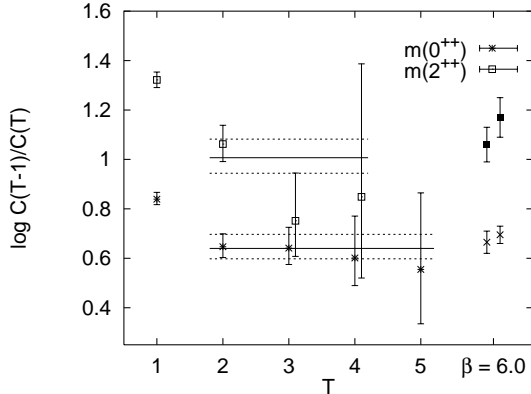


Figure 4. Effective glueball masses (fuzzing procedure 2).

In Figs. 3 and 4 we relate our $\kappa = 0.157$ results for glueball masses to those expected from quenched simulations at $\beta = 6.0$ [3,6], i.e. at similar lattice spacing ($a^{-1} \approx 2.1$ GeV). For

comparison, the quenched data points have been scaled by the ratio of the corresponding r_0 -values: 5.35/5.55 [5] within the figures. Again, the two fuzzing procedures yield consistent values.

Table 1

Torelon masses.

κ	$m(A_{1g})a$	$L_S a \kappa$	$2m_\pi a$
0.1560	0.80(7)	0.82(2)	0.890(2)
0.1570	0.68(8)	0.71(2)	0.677(2)
0.1575	0.58(4)	0.63(2)	0.576(9)

In Table 1, we have collected results of the torelon mass as extracted by use of fuzzing procedure 2 for all three κ values. For comparison, we have included the expectation from the (effective) slope of the interquark potential at large distance, κ [5], as well as the mass of two (non-interacting) π 's [7]. Note, that at $\kappa = 0.1575$ we are traversing the $\pi\pi$ threshold in the sense that the π turns lighter than half the torelon mass expectation from the potential. Thus, it is not clear whether our ground state still corresponds to the torelon or to a two pion state. This might explain why the torelon seems to become somewhat lighter than the expectation in this case.

Table 2

Glueball masses.

κ	$m(0^{++})a$	$m(2^{++})a$
0.1560	0.70(6)	1.14(12)
0.1570	0.64(5)	1.01 (7)
0.1575	0.56(6)	1.00 (7)

In Table 2 results for the scalar and tensor glueball masses are displayed. Note, that the value $m(0^{++})a = 0.56(6)$, obtained at $\kappa = 0.1575$, is consistent with $2m_\pi a = 0.58(1)$ [7], opening this decay channel. In Table 3, we compare unquenched with quenched results [3] obtained at $\beta = 6.0$ as well as quenched results from Refs. [1–3,6] that have been extrapolated to the continuum ($\beta = \infty$) quadratically in a . The scale r_0^{-1} from

Table 3
Comparison with quenched results.

κ	$m(0^{++})r_0$	$m(2^{++})/m(0^{++})$
0.1560	3.60(35)	1.62(21)
0.1570	3.55(33)	1.58(17)
0.1575	3.28(38)	1.78(21)
$\beta = 6.0$	3.69(23)	1.67(15)
$\beta = \infty$	4.22(14)	1.40(15)

the interquark potential corresponds to 400 MeV. All results are in agreement with the quenched data at $\beta = 6.0$. Deviations from the continuum limit are expected to depend linearly on a with dynamical Wilson quarks.

4. CONCLUSIONS

We have studied masses of the scalar and tensor glueballs as well as of the torelon with two flavours of Wilson quarks at $\beta = 5.6$. All results are consistent with those of quenched studies at similar lattice spacings. The statistical errors turn out to be encouraging and will compete with their quenched counterparts, once we have arrived at final statistics. Between $\kappa = 0.157$ and $\kappa = 0.1575$, corresponding to ratios $m_\pi/m_\rho = 0.76$ and 0.71 [7], the π becomes lighter than half the torelon mass and string breaking is expected to set in on $L_S = 16$ lattices. Around $\kappa \approx 0.1575$ the scalar glueball becomes unstable, which means that this region deserves further attention. Computations on $24^3 40$ lattices at $\kappa = 0.1575$ and $\kappa = 0.158$ are in progress.

ACKNOWLEDGEMENTS

The present work has been supported by DFG grants Schi 257/1-4 and Schi 257/3-2, EC project SC1*-CT91-0642 and EC contract CHRX-CT92-0051. GB acknowledges support by EU grant ERB CHBG CT94-0665.

REFERENCES

1. UKQCD collaboration: G.S. Bali, A. Hulsebos, A.C. Irving, Ch. Michael, K. Schilling and P. Stephenson, Phys. Lett. B309 (1993) 378.
2. GF11 collaboration: J. Sexton, A. Vaccarino and D. Weingarten, Phys. Rev. Lett. 75 (1995) 4563.
3. Ch. Michael and M. Teper, Nucl. Phys. B314 (1989) 347.
4. HEMCGC collaboration: K.M. Bitar *et al.*, Phys. Rev. D44 (1991) 2090; Nucl. Phys. B (Proc. Suppl.) 30 (1993) 315.
5. SESAM collaboration: U. Glässner, S. Güsken, H. Hoerber, Th. Lippert, G. Ritzenhöfer, K. Schilling, G. Siegert and A. Spitz, preprint HLRZ 96-20, hep-lat/9604014 (1996), Phys. Lett. B, in print.
6. UKQCD collaboration: G.S. Bali, A. Hulsebos, A.C. Irving, Ch. Michael, K. Schilling and P. Stephenson, unpublished.
7. U. Glässner for SESAM collaboration, preprint HLRZ 96/61, hep-lat/9608083, to be published in proceedings of Lattice '96.